

CRAMER-RAO BOUNDS FOR DATA-AIDED SAMPLING CLOCK OFFSET AND CHANNEL ESTIMATION

Sophie Gault, Walid Hachem

Service Radioélectricité, Supélec, France
 {sophie.gault,walid.hachem}@supelec.fr

Philippe Ciblat

Département Comélec, ENST, France
 philippe.ciblat@enst.fr

ABSTRACT

We derive the Cramer-Rao Bound (CRB) on the joint estimates of the sampling clock offset and the channel impulse response when a training sequence is available. Simple closed form expressions are obtained for the CRB in the case where the observation window is large, and furthermore in the case where the channel degree is large. Our derivations are suited for single-carrier as well as for multi-carrier Orthogonal Frequency Division Multiplexing (OFDM) schemes. Data-aided Maximum-Likelihood (ML) estimates are also carried out.

1. INTRODUCTION

For a digital communication system to work properly, the receiver's clock has to be synchronized with the transmitter's. Often, estimating the optimum sampling delay boils down to recovering the so-called constant symbol timing. Nevertheless, as soon as the transmit burst becomes very long or an OFDM system with a large number of subcarriers is considered, the clock frequency offset mismatch has to be taken into account. Indeed this offset leads to an linearly time-varying sampling delay over the entire observation window. For instance, in Very high speed Digital Subscriber Lines (VDSL) transmissions, even over the duration of one OFDM symbol, the clock frequency offset effect can not be neglected since the value of the product of the relative clock frequency offset with the number of carriers (that can reach respectively 10^{-4} and 4096 in VDSL [1]) is large ([2]). As an other example, Power Line Transmissions (PLT) in the band [1MHz, 20MHz] [3] show a similar behavior with respect to this phenomenon. The literature proposes several data-aided (*i.e.*, training sequence based) algorithms to perform the estimation of the clock frequency offset ([4, 5, 6, 7, 8]). Obviously, even if some authors assume the channel perfectly known at the receiver, it is more realistic, as done hereafter, to consider the joint estimation of the clock frequency offset and of the channel.

In order to benchmark the existing estimates, it is worth deriving the Cramer-Rao bound of the joint channel and clock frequency offset estimators. This will be the purpose of this paper.

In section 2 the signal model is presented. Section 3 is devoted to the derivation of the CRB. In section 4, we simplify the closed-form expressions of the CRB when the observation window length grows large as well as when the channel degree is large as it is usual in wireline applications (in VDSL and in PLT applications, the channel degree is often of order 100). In section 5 the ML estimator is presented together with a simplified version. Some numerical illustrations are drawn in section 6.

This work is supported by the French grant RNRT/IDILE.

2. MODEL

The continuous-time received signal $y_a(t)$ writes as follows :

$$y_a(t) = \sum_{k \in \mathbb{Z}} d_k g_a(t - kT) + b_a(t) \quad (1)$$

where $\{d_k\}_{k \in \mathbb{Z}}$ is the training sequence known to the receiver. The unknown impulse response $g_a(t)$ represents the complete channel that includes the transmit filter, the propagation channel, and the receiver low-pass filter. Throughout the paper, we assume that the filter $g_a(t)$ is time-limited and causal. Although unbounded in theory, the frequency support of $g_a(t)$ will in practice be assumed to coincide with $[-\rho/2T, \rho/2T]$ for some known parameter ρ . Finally $b_a(t)$ is an additive noise independent of the data.

Equation (1) models a large number of digital signals : in the case of standard single carrier modulated signals, $\{d_k\}_{k \in \mathbb{Z}}$ are the training symbols, T is the symbol rate, and ρ coincides with $1 + \alpha$ where α is the roll-off factor. In a multicarrier OFDM setting, $\{d_k\}_{k \in \mathbb{Z}}$ represents the output of the IFFT device, T is the sampling period, and $\rho \leq 1$.

If the transmitter and receiver clocks were perfectly synchronized, then the signal $y_a(t)$ would have been sampled at the period $T_s = T/q$, where $q \geq 1$ is an integer "oversampling factor" satisfying the conditions of the sampling theorem. In the absence of synchronization, $y_a(t)$ is sampled at $(1 + \delta)T_s$ instead of T_s , where δ is an unknown offset lying in the known interval $[-\delta_{\max}, \delta_{\max}]$. The discrete-time signal $y(n) = y_a(n(1 + \delta)T_s)$ thus writes

$$y(n) = \sum_{k \in \mathbb{Z}} d_k g_a(nT_s - kT + n\delta T_s) + b(n).$$

In the sequel, $b(n) = b_a((1 + \delta)nT_s)$ is assumed white Gaussian circular with zero-mean and known variance $\sigma^2 = \mathbb{E}[|b(n)|^2]$. Let $\{s_k\}_{k \in \mathbb{Z}}$ be the sequence defined as $s_k = d_{k/q}$ if $k/q \in \mathbb{Z}$, and $s_k = 0$ otherwise. The previous equation then takes the following form

$$y(n) = \sum_{k \in \mathbb{Z}} s_k g_a((n - k + n\delta)T_s) + b(n).$$

Because $g_a(t)$ is band-limited, it can be written as

$$g_a(t) = \sum_{l \in \mathbb{Z}} h_l p_a(t - lT_s)$$

where $p_a(t)$ is any interpolation filter with $\rho/2T$ as a cut-off frequency ([9]). As $g_a(t)$ is time-limited, $p_a(t)$ is assumed time-supported by $[0, MT_s]$ and the sequence $\{h_l\}_{l \in \mathbb{Z}}$ is assumed finite with length $L + 1$.

The paper focuses on the joint estimation of the sampling clock

offset δ and of the channel impulse response $\mathbf{g} = [g_0, \dots, g_{L+M}]^T$ with $g_l = g_a(lT_s)$. Clearly the interpolator $p_a(t)$ is available at the receiver while the vector $\mathbf{h} = [h_0, \dots, h_L]^T$ is not.

3. EXACT CRAMER-RAO BOUND

NT_s being the duration of the observation window, we have

$$y(n) = \sum_{k=-K_N}^{K_N+M} \sum_{l=0}^L h_l s_{n-k-l} p(k+n\delta) + b(n) \quad (2)$$

where $p(u) = p_a(uT_s)$ and K_N is the smallest integer such that $K_N \geq N\delta_{\max}$. The aim of the section is to derive CRB on $[\tilde{\mathbf{g}}^T, \delta]^T$ where $\tilde{\mathbf{g}} = [\Re[\mathbf{g}^T], \Im[\mathbf{g}^T]]^T$. Notations $\Re[\cdot]$ and $\Im[\cdot]$ stand for real and imaginary parts of a complex-valued matrix respectively. By setting $\mathbf{y}_N = [y(0), \dots, y(N-1)]^T$, equation (2) can be put in a matrix form :

$$\mathbf{y}_N = \mathbf{S}_N \mathbf{P}_N(\delta) \mathbf{h} + \mathbf{b}_N \quad (3)$$

where

$$\mathbf{S}_N = \begin{bmatrix} s_0 & & 0 \\ & \ddots & \\ 0 & & s_{N-1} \end{bmatrix}, \quad \mathbf{P}_N(\delta) = \begin{bmatrix} p(0) \\ \vdots \\ p((N-1)\delta) \end{bmatrix},$$

with $\mathbf{s}_n = [s_{n+K_N}, \dots, s_{n-(M+K_N)-L}]$ and with $\mathbf{p}(n\delta)$ being the $(2K_N + M + L + 1) \times (L + 1)$ Toeplitz matrix having $[p(n\delta - K_N), 0, \dots, 0]$ as its first row and $[p(n\delta - K_N), \dots, p(n\delta + K_N + M), 0, \dots, 0]^T$ as its first column.

The vector \mathbf{y}_N is circular multivariate Gaussian process with unknown mean $\boldsymbol{\mu} = \mathbf{S}_N \mathbf{P}_N(\delta) \mathbf{h}$ and known covariance matrix $\sigma^2 \mathbf{I}_N$. At this point, we need the expression of the Fisher Information Matrix (FIM) on the parameter vector $\boldsymbol{\theta} = [\theta_0, \dots, \theta_{2(L+1)}]^T = [\tilde{\mathbf{h}}^T, \delta]^T$ where $\tilde{\mathbf{h}} = [\Re[\mathbf{h}^T], \Im[\mathbf{h}^T]]^T$. Following [10], the FIM expresses as follows

$$\mathbf{F}_N = \frac{2}{\sigma^2} \Re \left[\frac{\partial \boldsymbol{\mu}^H}{\partial \boldsymbol{\theta}} \cdot \frac{\partial \boldsymbol{\mu}}{\partial \boldsymbol{\theta}} \right]$$

with $\frac{\partial \boldsymbol{\mu}}{\partial \boldsymbol{\theta}} = [\frac{\partial \boldsymbol{\mu}}{\partial \theta_0}, \dots, \frac{\partial \boldsymbol{\mu}}{\partial \theta_{2(L+1)}}]$. One can easily show that

$$\mathbf{F}_N = \frac{2}{\sigma^2} \begin{bmatrix} N \Re[\mathbf{U}_N] & -N \Im[\mathbf{U}_N] & N^2 \Re[\mathbf{V}_N \mathbf{h}] \\ N \Im[\mathbf{U}_N] & N \Re[\mathbf{U}_N] & N^2 \Im[\mathbf{V}_N \mathbf{h}] \\ N^2 \Re[\mathbf{h}^H \mathbf{V}_N^H] & -N^2 \Im[\mathbf{h}^H \mathbf{V}_N^H] & N^3 \mathbf{h}^H \mathbf{W}_N \mathbf{h} \end{bmatrix}$$

where

$$\begin{aligned} \mathbf{U}_N &= \frac{1}{N} \mathbf{P}_N^T(\delta) \mathbf{S}_N^H \mathbf{S}_N \mathbf{P}_N(\delta) \\ \mathbf{V}_N &= \frac{1}{N^2} \mathbf{P}_N^T(\delta) \mathbf{S}_N^H \mathbf{S}_N \mathbf{Q}_N(\delta) \\ \mathbf{W}_N &= \frac{1}{N^3} \mathbf{Q}_N^T(\delta) \mathbf{S}_N^H \mathbf{S}_N \mathbf{Q}_N(\delta) \end{aligned}$$

with $\mathbf{Q}_N(\delta) = d\mathbf{P}_N(\delta)/d\delta$. The reason for introducing the factors $1/N$, $1/N^2$, and $1/N^3$ will become apparent in the next paragraph. By applying the well known formulas for the inversion of block partitioned matrices, we obtain :

$$\mathbf{F}_N^{-1} = \begin{bmatrix} \mathbf{A}_N & \mathbf{b}_N \\ \mathbf{b}_N^T & c_N \end{bmatrix}$$

where

$$\mathbf{A}_N = \frac{\sigma^2}{2N} \left(\begin{bmatrix} \Re[\mathbf{U}_N^{-1}] & -\Im[\mathbf{U}_N^{-1}] \\ \Im[\mathbf{U}_N^{-1}] & \Re[\mathbf{U}_N^{-1}] \end{bmatrix} + \frac{1}{\gamma_N} \begin{bmatrix} \Re[\boldsymbol{\beta}_N] \\ \Im[\boldsymbol{\beta}_N] \end{bmatrix} \begin{bmatrix} \Re[\boldsymbol{\beta}_N^T] & \Im[\boldsymbol{\beta}_N^T] \end{bmatrix} \right) \quad (4)$$

$$\mathbf{b}_N = -\frac{\sigma^2}{2N^2 \gamma_N} \begin{bmatrix} \Re[\boldsymbol{\beta}_N] \\ \Im[\boldsymbol{\beta}_N] \end{bmatrix} \quad (5)$$

$$c_N = \frac{\sigma^2}{2N^3 \gamma_N} \quad (6)$$

$$\boldsymbol{\beta}_N = \mathbf{U}_N^{-1} \mathbf{V}_N \mathbf{h}, \text{ and} \quad (7)$$

$$\gamma_N = \mathbf{h}^H (\mathbf{W}_N - \mathbf{V}_N^H \mathbf{U}_N^{-1} \mathbf{V}_N) \mathbf{h}. \quad (8)$$

One can notice that $\mathbf{g} = \mathbf{P} \mathbf{h}$ where \mathbf{P} is the $(L+M+1) \times (L+1)$ Toeplitz matrix with first row $[p(0), 0, \dots, 0]$ and first column $[p(0), \dots, p(M), 0, \dots, 0]^T$. Therefore the CRB on $[\tilde{\mathbf{g}}^T, \delta]^T$ expresses as follows

$$\begin{bmatrix} \text{CRB}_N^{(\mathbf{g}, \mathbf{g})} & \text{CRB}_N^{(\mathbf{g}, \delta)} \\ \text{CRB}_N^{(\delta, \mathbf{g})} & \text{CRB}_N^{(\delta, \delta)} \end{bmatrix} = \begin{bmatrix} \tilde{\mathbf{P}} \mathbf{A}_N \tilde{\mathbf{P}}^T & \tilde{\mathbf{P}} \mathbf{b}_N \\ \mathbf{b}_N^T \tilde{\mathbf{P}}^T & c_N \end{bmatrix}$$

where $\tilde{\mathbf{P}} = [\mathbf{P}, \mathbf{0}; \mathbf{0}, \mathbf{P}]$. In particular, we have

$$\mathbb{E} [\|\tilde{\mathbf{g}}_N - \mathbf{g}\|^2] \geq \frac{\sigma^2}{2N} \left(2\text{tr}(\mathbf{P} \mathbf{U}_N^{-1} \mathbf{P}^T) + \frac{\boldsymbol{\beta}_N^H \mathbf{P}^T \mathbf{P} \boldsymbol{\beta}_N}{\gamma_N} \right) \quad (9)$$

4. ASYMPTOTIC CRAMER-RAO BOUND

4.1. Asymptotic Behavior for Long Training Sequences

Hereafter, $(d_k)_{k \in \mathbb{Z}}$ is assumed a stationary process with the power spectral density $S_d(e^{2i\pi f})$. Hence, $(s_k)_{k \in \mathbb{Z}}$ is cyclostationary, and its cyclic spectral density $S_s^{(0)}(e^{2i\pi f})$ at cycle 0 is equal to

$$S_s^{(0)}(e^{2i\pi f}) = \frac{1}{q} S_d(e^{2i\pi qf}). \quad (10)$$

Write $n\delta = \text{int}[n\delta] + \text{rem}[n\delta]$ where $\text{int}[n\delta]$ is the largest integer less than or equal to $n\delta$. Then one can verify that the entries of matrix $\mathbf{U}_N = \{u_N(l, l')\}_{0 \leq l, l' \leq L}$ are given by

$$u_N(l, l') = \frac{1}{N} \sum_{m, m' n=0}^N \frac{s_{n+\text{int}[n\delta]-m-l} s_{n+\text{int}[n\delta]-m'-l'}}{p(\text{rem}[n\delta] + m) p(\text{rem}[n\delta] + m')}.$$

Here, it can be shown with a mild mixing condition on (d_k) that

$$u_N(l, l') \xrightarrow{\text{a.s.}} \underbrace{\sum_m R_s^{(0)}(m+l-l') \int_{-\infty}^{+\infty} p(t) p(t-m) dt}_{u(l, l')}$$

where $\xrightarrow{\text{a.s.}}$ stands for the almost sure convergence and $R_s^{(0)}(\tau)$ denotes the cyclic correlation function of s at cycle 0. The proof includes a discussion on whether δ is irrational or not. It will be skipped here for lack of space.

It will be convenient to express $u(l, l')$ in the frequency domain. Denote by $P(f)$ the Fourier transform of $p(t) = p_a(tT_s)$. From Parseval's identity and using (10), we get

$$u(l, l') = \frac{1}{q} \int_{-\infty}^{\infty} |P(f)|^2 S_d(e^{2i\pi qf}) e^{2i\pi f(l-l')} df.$$

Finally we obtain

$$\mathbf{U} = \frac{1}{q} \int_{-\infty}^{\infty} |P(f)|^2 S_d(e^{2i\pi qf}) \mathbf{d}_L(e^{2i\pi f}) \mathbf{d}_L^H(e^{2i\pi f}) df \quad (11)$$

where $\mathbf{d}_L(e^{2i\pi f}) = [1, \dots, e^{2i\pi fL}]^T$. From similar derivations, the almost sure limits of \mathbf{V}_N and \mathbf{W}_N express respectively as

$$\mathbf{V} = \frac{-i\pi}{q} \int_{-\infty}^{\infty} f |P(f)|^2 S_d(e^{2i\pi qf}) \mathbf{d}_L(e^{2i\pi f}) \mathbf{d}_L^H(e^{2i\pi f}) df \quad (12)$$

$$\mathbf{W} = \frac{4\pi^2}{3q} \int_{-\infty}^{\infty} f^2 |P(f)|^2 S_d(e^{2i\pi qf}) \mathbf{d}_L(e^{2i\pi f}) \mathbf{d}_L^H(e^{2i\pi f}) df. \quad (13)$$

Since matrices \mathbf{U}_N , \mathbf{V}_N , and \mathbf{W}_N converge as $N \rightarrow \infty$, the mean-square errors for the channel and the sampling clock offset are of order $\mathcal{O}(1/N)$ and $\mathcal{O}(1/N^3)$ respectively (see (9) and (6)).

4.2. Asymptotic Behavior for Long Channels

In order to obtain more compact CRB expressions, we now study the asymptotic regime where $L \rightarrow \infty$, $N \rightarrow \infty$ and $L/N \rightarrow 0$, and make profit of the Toeplitz nature of \mathbf{U} , \mathbf{V} , and \mathbf{W} .

Because of the band-limited nature of $P(f)$, the integration in (11–13) can in practice be done over $[-\rho/2q; \rho/2q]$, the effective band of $p(t)$. Assuming that $S_d(e^{2i\pi qf})$ does not vanish on this interval, \mathbf{U} is numerically singular with an effective rank close to $\text{int}[\rho L/q]$ ([11, chap. 7]). Let the singular value decomposition of \mathbf{U} be

$$\mathbf{U} = [\mathbf{E}_1 \ \mathbf{E}_2] \begin{bmatrix} \Sigma_1 & 0 \\ 0 & \Sigma_2 \end{bmatrix} [\mathbf{E}_1 \ \mathbf{E}_2]^H$$

where Σ_1 is the diagonal matrix bearing on its diagonal the dominant eigenvalues, *i.e.* those corresponding to the non-negligible values of the integrand in (11). With a small notation abuse, we denote by $\mathbf{U}^\#$ the “pseudo-inverse” matrix $\mathbf{E}_1 \Sigma_1^{-1} \mathbf{E}_1^H$. One can prove here [12] that $\|\mathbf{P}\mathbf{E}_2\| \approx 0$. Therefore, as is implicitly done in [13], the matrix \mathbf{U}^{-1} can be replaced with $\mathbf{U}^\#$ in the CRB expressions for $[\hat{\mathbf{g}}^T, \delta]^T$. We therefore have

$$\frac{N}{L} \mathbb{E} [\|\hat{\mathbf{g}}_N - \mathbf{g}\|^2] \geq \frac{\sigma^2}{L} \text{tr}(\mathbf{P}\mathbf{U}^\#\mathbf{P}^T) + \mathcal{O}\left(\frac{1}{L}\right),$$

and in a similar manner

$$N^3 \mathbb{E} [|\hat{\delta}_N - \delta|^2] \geq \frac{\sigma^2}{2\mathbf{h}^H (\mathbf{W} - \mathbf{V}^H \mathbf{U}^\# \mathbf{V}) \mathbf{h}}.$$

Using some known results about asymptotic behavior of Toeplitz matrices ([11]), it can be shown that in the asymptotic regime,

$$\frac{N}{L} \mathbb{E} [\|\hat{\mathbf{g}}_N - \mathbf{g}\|^2] \gtrsim \sigma^2 \int_{-\rho/2}^{\rho/2} \frac{1}{S_d(e^{2i\pi qf})} df$$

and

$$N^3 \mathbb{E} [|\hat{\delta}_N - \delta|^2] \gtrsim \frac{3q\sigma^2}{2\pi^2 \int_{-\frac{\rho}{2q}}^{\frac{\rho}{2q}} f^2 |h(e^{2i\pi f})|^2 |P(f)|^2 S_d(e^{2i\pi qf}) df}$$

where $h(z) = \sum_{l=0}^L h_l z^{-l}$. For lack of space, technical details are omitted.

By inspecting these two expressions, one notices that when the

training sequence is white in the useful frequency band, the CRB for the channel estimation is minimum. As for the clock frequency offset CRB, due to the term f^2 in the integral, it is worth attributing a large amount of power to the high frequencies except if the channel fading for these frequencies is too strong.

5. ML ESTIMATION

Let us get back to our model (3) as both the number of samples and the filter degree are finite. The Log-Likelihood function $\mathcal{L}(\boldsymbol{\theta})$ to be minimized takes the following form :

$$\mathcal{L}(\boldsymbol{\theta}) = \|\mathbf{y}_N - \mathbf{S}_N \mathbf{P}_N(\delta) \mathbf{h}\|^2$$

The minimization of $\mathcal{L}(\boldsymbol{\theta})$ leads to the following ML based estimates of δ and \mathbf{g} ([14],[10]) :

$$\begin{cases} \hat{\delta}_N &= \arg \max_{\delta} \mathbf{y}_N^H \boldsymbol{\Pi}_N(\delta) \mathbf{y}_N \\ \hat{\mathbf{h}}_N &= \left(\mathbf{P}_N^T(\hat{\delta}_N) \mathbf{S}_N^H \mathbf{S}_N \mathbf{P}_N(\hat{\delta}_N) \right)^{-1} \mathbf{P}_N^T(\hat{\delta}_N) \mathbf{S}_N^H \mathbf{y}_N \\ \hat{\mathbf{g}}_N &= \mathbf{P} \hat{\mathbf{h}}_N \end{cases}$$

where

$$\boldsymbol{\Pi}_N(\delta) = \mathbf{S}_N \mathbf{P}_N(\delta) \left(\mathbf{P}_N^T(\delta) \mathbf{S}_N^H \mathbf{S}_N \mathbf{P}_N(\delta) \right)^{-1} \mathbf{P}_N^T(\delta) \mathbf{S}_N^H.$$

In order to compute the ML based sampling clock offset estimate, an exhaustive search has to be carried out. As each try of a value of δ requires a matrix inversion, the implementation of this algorithm is impractical. The estimates can however be greatly simplified in the asymptotic regime of section 4.2. $\boldsymbol{\Pi}_N(\delta)$ can be replaced with

$$\underline{\boldsymbol{\Pi}}_N(\delta) = \frac{1}{N} \mathbf{S}_N \mathbf{P}_N(\delta) \mathbf{U}^\# \mathbf{P}_N^T(\delta) \mathbf{S}_N^H.$$

Notice that the pseudo-inversion becomes independent of δ and so can be done only once. Notice also that, due to the pseudo-inversion, we are only able to estimate the projection of \mathbf{h} on the column space of \mathbf{E}_1 , which corresponds to the in-band part of $h(e^{2i\pi f})$. Nevertheless as the parameter of interest is \mathbf{g} , values of $h(e^{2i\pi f})$ out of the band are not needed, and therefore the estimate of \mathbf{g} remains accurate. Here, the estimation algorithm becomes

$$\begin{cases} \hat{\delta}_N &= \arg \max_{\delta} \mathbf{y}_N^H \underline{\boldsymbol{\Pi}}_N(\delta) \mathbf{y}_N \\ \hat{\mathbf{g}}_N &= \frac{1}{N} \mathbf{P} \mathbf{U}^\# \mathbf{P}_N^T(\hat{\delta}_N) \mathbf{S}_N^H \mathbf{y}_N \end{cases}$$

6. NUMERICAL ILLUSTRATIONS

Simulations are carried out in a single carrier context. The training sequence $\{d_k\}$ is a QPSK constellation based pseudo-random white sequence. The channel, provided to the authors by “Electricité de France”, is a power line channel in the band [1MHz; 20.5MHz]. The symbol rate is 16MHz, the transmission filter is a root raised cosine filter with a roll-off factor of 0.22, and $\delta = 7.10^{-5}$. Fig.1 shows the real and the imaginary parts of the first 80 samples of the equivalent base-band channel, obtained with an oversampling factor $q = 2$.

Fig.2 displays the CRB on δ and \mathbf{g} given by (6) and (9), their asymptotic values (§4.2), and the mean square errors of the simplified ML estimates (§5). Here, N varies from 200 to 5000 and the Signal to Noise Ratio (SNR) is 20dB. The asymptotic approximations of §4.2 appear reliable for $N \approx 1000$. In fig. 3, the same quantities are displayed versus the SNR, N being fixed to 2000. The variances of the sampling clock offset estimate and the channel estimate are of order $\mathcal{O}(1/\text{SNR})$. The simplified ML estimator is close to the asymptotic CRB for all these SNRs.

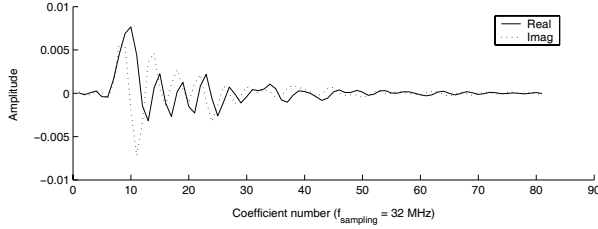


Fig. 1. Coefficients of the channel impulse response.

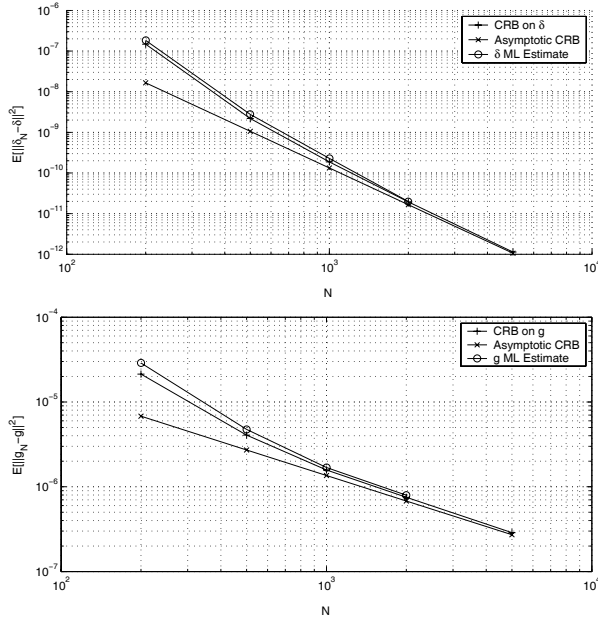


Fig. 2. Cramer-Rao bound on δ and g vs. N .

7. REFERENCES

- [1] ETSI, *Transmission and Multiplexing (TM); Access transmission systems on metallic access cables; Very high speed Digital Subscriber Line (VDSL); Part 2: Transceiver specification*, 2002–2002, TS 101 270-2.
- [2] T. Pollet, P. Spruyt, and M. Moeneclaey, “The BER Performance of OFDM Systems Using Non-Synchronized Sampling,” in *Proc. GLOBECOM*, 1994, pp. 253–257.
- [3] F.J. Cañete, J.A. Cortés, L. Díez, and J.T. Entrambasaguas, “Modeling and Evaluation of the Indoor Power Line Transmission Medium,” *IEEE Comm. Mag.*, vol. 41, no. 4, pp. 41–47, Apr. 2003.
- [4] B. Yang, Z. Ma, and Z. Cao, “ML-Oriented DA Sampling Clock Synchronization for OFDM Systems,” in *Proc. WCC/ICCT*, 2000, pp. 781–784.
- [5] L. Shou-Yin and C. Jong-Wha, “A study of joint tracking algorithms of carrier frequency offset and sampling clock offset for OFDM-based WLANs,” in *IEEE International Conference on Communications, Circuits and Systems and West Sino Expositions*, 2002, vol. 1, pp. 109–113.

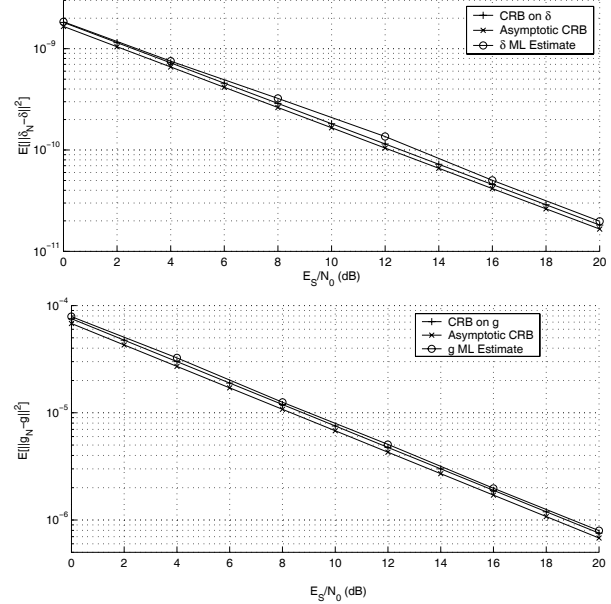


Fig. 3. Cramer-Rao bound on δ and g vs. SNR.

- [6] R. Heaton, S. Duncan, and B. Hodson, “A fine frequency and fine sample clock estimation technique for OFDM systems,” in *IEEE Vehicular Technology Conference (VTC)*, 2001, pp. 678–682.
- [7] K. Bucket and M. Moeneclaey, “Tracking performance of feedback timing synchronizer operating on interpolated signals,” in *IEEE Global Telecommunications Conference (GLOBECOM)*, 1996, pp. 67–71.
- [8] B. Yang, K. Letaief, R. Cheng, and Z. Cao, “An Improved Combined Symbol and Sampling Synchronization Method for OFDM Systems,” in *Proc. WCNC*, 1999, vol. 3, pp. 1153–1157.
- [9] J. Ayadi and D. Slock, “Cramer-Rao bounds and methods for knowledge based estimation of multiple FIR channel,” *Workshop SPAWC*, 1997.
- [10] O. Besson and P. Stoica, “Training sequence selection for frequency offset estimation in frequency selective channels,” *Digital Signal Processing*, vol. 13, pp. 106–127, 2003.
- [11] U. Grenander and G. Szegő, *Toeplitz Forms and their Applications*, Univ. of California Press, Berkeley, 1958.
- [12] D. Slepian, “Prolate spheroidal wave functions, fourier analysis and uncertainty,” *Bell System Technical Journal*, vol. 57, no. 5, May 1978.
- [13] P. Stoica and T. Marzetta, “Parameter estimation problems with singular information matrices,” *IEEE Trans. on SP*, vol. 49, no. 1, pp. 87–90, Jan. 2001.
- [14] M. Morelli and U. Mengali, “Carrier frequency estimation for transmissions over selective channels,” *IEEE Trans. on Communications*, vol. 48, no. 9, pp. 1580–1589, Sept. 2000.